*Physics – Uspekhi* **65** (5) 440 – 452 (2022) 

***PHYSICS OF OUR DAYS***

PACS numbers: 07.05.Mh, **82.40. – g**, **84.35. + i**

# Networks of spike oscillators and their application for creating autonomous intelligent devices

V K Vanag

DOI: https://doi.org/10.3367/UFNe.2021.05.038978

## Contents



**Abstract. Hierarchical networks of pulse-coupled chemical micro-oscillators (MOs) are considered. The Belousov–Zhabotinsky oscillatory reaction in a microvolume serves as a single MO. Biological principles of neural networks and the laws of nonlinear dynamics are used to operate the considered networks, which we call a 'chemical brain.' It has been shown that this 'chemical brain' is capable of adaptive behavior and decision-making.**

**Keywords:** networks of spike micro-oscillators, Belousov–Zhabotinsky reaction, decision-making, 'chemical brain'

**Abbreviations used:**
AOT — reverse (inverted) aerosol OT-microemulsion, OT stands for a trademark;
BZ — Belousov–Zhabotinsky reaction;
BZC solution — catalyst-free BZ solution
AI — artificial intelligence;
MA — malonic acid;
MO — microoscillator;
CFUR — continuously fed unstirred reactor;
CSTR — continuous stirred tank reactor;
FKN — Field–Köres–Noyes mechanism;
FIS — ferrocyanide–iodate–sulfite reaction system;
CIMA — chlorite–iodide–malonic acid reaction system;
AP — antiphase mode, out-of-phase oscillations;
AIP — almost in-phase oscillations of two oscillators;
CPG — central pattern generator, central rhythm generator;
DM — decision-making block;
E — executer;
FAP — fast antiphase oscillation;
IP — in-phase oscillation;
IPAP — in-phase antiphase, a mode that occurs in a system of four coupled oscillators;
OSI — a mode in which one oscillator is suppressed (S — suppressed) and is in a stationary oxidized state while the second oscillator is in an oscillatory regime (O — oscillatory);
OSII — a mode in which one oscillator is suppressed (S — suppressed) and is in a stationary excited state while the second oscillator is in an oscillatory regime;
PRC — phase response curve;
R — reader;
W — walk;
WR — walk reverse

**V K Vanag**
Center for Nonlinear Chemistry,
Immanuel Kant Baltic Federal University,
ul. A Nevskogo 14, 236016 Kaliningrad, Russian Federation
E-mail: vvanag@kantiana.ru

Received 30 March 2021
*Uspekhi Fizicheskikh Nauk* **192** (5) 477 – 490 (2022)
Translated by Yu V Morozov

## 1. Introduction

Some researchers believe that humankind is approaching the end of the era of 'silicon computers'; therefore, alternative computing systems will soon be needed, such as networks of coupled oscillators that provide the natural environment for parallel processing of information and may compete, in the future, with habitual von Neumann computers both in speed and energy efficiency [1, 2].

Networks of coupled oscillators have received increasing attention in recent years. They are studied and exploited by specialists engaged in different fields of research and science, viz. physicists, neurophysiologists, nonlinear chemists (as chemists concerned with nonlinear dynamics of chemical reactions are usually called), biophysicists, mathematicians (including those involved in discrete mathematics problem

solving), and experts in artificial intelligence, as well as amateurs interested in the latest scientific achievements. This list of specialists, even though incomplete, reflects the interdisciplinary nature of the topic of 'networks of coupled oscillators' and suggests a differential approach to its handling in relation to the goals and objectives of the work. As a biophysicist who has long dwelt on nonlinear (oscillatory) chemical reactions and has eventually become a nonlinear chemist, I find it important to briefly describe the evolutionary development of nonlinear chemistry that has led many to study networks of coupled oscillators.

The starting point is the discovery of the Belousov–Zhabotinsky (BZ) oscillating chemical reaction [3, 4]. It was this discovery and Prigogine's theory [5, 6] that gave rise to the boom in nonlinear chemistry [7–13]. Five Soviet scientists, G R Ivanitsky, V I Krinsky, A N Zaikin, A M Zhabotinsky, and B N Belousov, were awarded the Lenin Prize in 1980 ''for the discovery of a new class of autowave processes and the study of their role in disturbing stability of excitable distributed systems.'' Autowave processes in this formulation are understood as chemical waves in a spatially distributed BZ reaction. Three years earlier (1977), I R Prigogine received the Nobel Prize in chemistry ''for his contributions to nonequilibrium thermodynamics, particularly the theory of dissipative structures.''

These events gave an impetus to the avalanche-like increase in research activities concerning 'point' chemical oscillatory systems [7–10]. The word 'point' (i.e., an entity of zero dimensions like that of a point) refers to chemical reactions occurring in a well-stirred chemical reactor system continuously fed with fresh reagents. Dozens of new oscillatory reactions were discovered; in fact, the total number reaches hundreds if various modifications of these reactions are taken into account. Their main types, apart from the BZ reaction, include the CHIM (chlorite–iodide–malonic acid) reaction [14], pH oscillators [15, 16], and a particular case of pH oscillators referred to as the ferrocyanide–iodate–sulfite (FIS) reaction [17–19] and held to be of importance due to the formation of dissipative spatial structures in special two-dimensional reactors where this reaction proceeds.

In the course of this work, the basic rules and patterns were discovered that underlie the generation of oscillatory modes in chemical reactions, the transition from the bistability mode to the oscillatory one [20], the presence of positive and negative feedback, as well as the time delay between the moments of maximum manifestation of these two types of connections [21, 22]. Speaking mathematically, they are the chemical-kinetic conditions for the appearance of the Andronov–Hopf bifurcation that follow from the analysis of the Jacobian eigenvalues of the linearized system [5]. In the case of subcritical Hopf bifurcation, low-amplitude sinusoidal (harmonic) oscillations appear, while supercritical Hopf bifurcation gives rise to high-amplitude relaxation oscillations [23]. Relaxation oscillations are directly related to the concept of 'spike oscillators' on which we shall dwell in this review. In neurophysiology, a spike is understood as the rapid excitation of a neuron and the passage of the action potential along the axon. The explosive excitation of the oscillator in the case of relaxation oscillations resembles the appearance of a spike. Unlike harmonic oscillations, each period of relaxation oscillations can be divided into two distinct stages: fast and slow changes in the state of the system. The stage of fast and short-term changes with a pronounced peak (the maximum change in the state of the system) is called a spike.

Following the early stage of the study of point oscillating systems, nonlinear chemistry entered the stage of research on 'dissipative structures.' It cannot be definitely asserted that the initial stage of investigation into point oscillatory systems was directly followed by the next stage of studying dissipative structures in spatially distributed systems. Indeed, these stages are superimposed at the time scale; nevertheless, they are readily distinguishable in the historical process of the development of nonlinear chemistry. The stage of studying 'dissipative structures' began with the invention of continuously fed unstirred reactors (CFURs) [24] and the experimental discovery of Turing structures [25, 26]. Almost 40 years passed since the prediction of stationary dissipative structures by Alan Turing [27] and their observation in experiment.

The invention of CFURs raised the level of research on chemical waves carried out since their discovery by A N Zaikin and A M Zhabotinsky [28]. Earlier, they were regarded as waves in a closed system and therefore unstable in time. CFURs made it possible to maintain these structures for an arbitrarily long time. This led to a whole series of discoveries of new subtler wave phenomena, such as superspirals [29] and long-wavelength instability [30, 31]. In the early 2000s, new dissipative structures were found in the so-called BZ-AOT system in which the BZ reaction proceeds not in an aqueous solution but in a reverse (inverted) aerosol microemulsion (AOT) [32]. Such structures include antiwaves [33], packet waves [34], segment waves [35], oscillon [36], and new types of Turing structures [37–39].

However, by the end of the first decade of the 2000s, nonlinear chemists' interest began to switch to the study of large and small ensembles of coupled oscillators. Of course, coupled oscillators attracted the attention of researchers much earlier than that, but the appearance of chemical microoscillators about 10 years ago made possible experimental studies of ensembles of coupled MOs [40, 41]. There are a small number of scientific groups in the world that are able to carry out such experiments. First of all, there is the group of Professor Showalter from the University of West Virginia (USA) [42–45] and the group of Professor Taylor from the University of Sheffield (UK) [46–48], two groups from Brandeis University (USA) (one headed by Professor Epstein [40, 41, 49, 50] and the other by Professor Fraden [51, 52]), the group of Professor Gorecki in Warsaw (Institute of Physical Chemistry, Polish Academy of Sciences) closely collaborating with the group of Professor Adamatzky from the University of the West of England, Bristol [53–55], the group of professor Rossi in Italy (Università degli Studi di Siena) [56, 57], the group of professor Yoshikawa (Japan) [58–60], and our group from Immanuel Kant Baltic Federal University (Russia) [61–63].

A large number of chemical MOs is not yet a network of oscillators. They need to be connected by short-range (i.e. diffusive) or long-range (i.e., impulsive) forces. In the second decade of the 2000s, a method for pulse coupling with a time delay between two chemical oscillators [64, 65] and an optical method for establishing a pulse coupling between BZ MOs with the immobilized photosensitive catalyst $Ru(bpy)_3^{2+}$ [66] were proposed. These techniques made it possible to start experimental investigations into networks of pulse-coupled chemical MOs.

The path of mathematicians and theoretical physicists to knowledge of networks of coupled oscillators was much

shorter, because many of them passed the stage of dissipative spatially distributed structures and immediately switched from point oscillators to their ensembles [67–71]. The birth of the theory of neural networks is assumed to date to 1959 [72], i.e., it preceded the discovery of oscillations in the BZ reaction, but occurred later than the famous work of Hodgkin and Huxley on the propagation of an electrical signal along the axon [73]. With the increase in the counting speed of computers, it became possible to solve dynamic problems involving hundreds and thousands of coupled oscillators; also, this promoted the extension of research on network problems. Finally (if not primarily), the mysteries of the functioning of the brain, which consists of a huge number of coupled oscillators and excitable cells (neurons), support the continued interest of the scientific community in the problems associated with networks of active elements.

This review is designed to present relatively new networks of spike oscillators in which a single oscillator is a chemical oscillatory reaction occurring in a microvolume. In contrast to previous work in which the dynamic regimes of MO networks were studied, we wish to show that new hierarchical networks are also capable of performing some 'intelligent' operations related to adaptation to external signals and decision-making. Networks of chemical MOs can operate without electricity using 'chemical fuel' alone. The review is divided into several sections. In Section 2, we consider ways to classify various networks of oscillators and active elements. Section 3 is focused on neural networks and discusses the possibility of using the principles of their operation to create artificial networks of chemical MOs. Section 4 describes MOs based on the Belousov–Zhabotinsky (BZ) reaction. Section 5 is intended to describe pulse coupling with time delay and a detailed analysis of its characteristics. Dynamic modes of BZ MOs coupled by diffusion or impulsive forces are considered in Section 6. Small networks of spike oscillators, clustering, multirhythms, and the formation of functional hierarchy are dealt with in Section 7. Section 8 is devoted to the principles of operation of the 'chemical brain.' In Section 9, we discuss the operation of the central decision-making block which endows the networks of coupled oscillators with 'intelligence.' The review ends with a short conclusion and the assessment of further prospects for research (Section 10).

## 2. Classification of networks

Networks of coupled oscillators can be classified according to several criteria, for example, by the type of differential equations describing the dynamics of a single oscillator: a network can consist of the simplest phase oscillators [70, 74] or complete models of real (chemical or neurophysiological) oscillators [75]. Also, classification can be based on the network topology, e.g., links of oscillators with each other, links only with the nearest neighbors, or links like those in the small-world model [76]. Finally, it can take into account the architectural complexity inherent in hierarchical networks [62, 77] or be focused on the type of connections between network nodes (i.e., oscillators). These can be either local diffusive connections, as between chemical MOs [40], or long-range pulse coupling similar to connections between neurons through axons and dendrites [64]. In a real neural network, local diffusion connections correspond to electrical synapses (contacts) between neighboring cells. Neurophysiologists note that both types of connections, impulsive (i.e., chemical synapses) and diffusive (electrical synapses) coupling, are important for the functioning of the nervous system, even in primitive invertebrates [78, 79]. The coupling can be either inhibitory (i.e., suppressive) or excitatory (via an activator) [64, 80], with or without time delay [81], unidirectional or mutual, constant or adjustable (i.e., changing over time) [82]. Only pulse coupling can be unidirectional, whereas diffusive coupling is obviously bidirectional (i.e., reciprocal). The literature on artificial neural networks also distinguishes between recurrent networks and so-called 'feedforward' networks [83]. There are no feedback loops in networks of the latter type, although all their elements are interconnected and information is transmitted only in one direction, from inputs to outputs. The classical perceptron belongs to this class of networks [84, 85]. Such classification of networks may not give an answer to the question about the dependence of dynamic modes of a network on its architecture, but there is still no deeper classification providing a prediction of dynamic modes based on topology.

## 3. Neural networks

There is a very extensive literature on networks of coupled oscillators and excitable elements (see, for example, the review co-authored by the well-known Professor Ermentrout [86]). However, little progress has thus far been made in understanding how the brain works [87]. Well-known neurophysiologists insist on the necessity of combining empirical and theoretical approaches [87–89]. Such an appeal sounds a bit strange to physicists who believe such an approach to be the only way to address a problem. Hopes that the identification of all connections between brain neurons ('connectome' [90–92]) would make it possible to understand how the brain works have gone. Even determination of the structure of all interneuronal connections in the simplest nervous system of the nematode *Caenorhabditis elegans* composed of 302 neurons [93] did not provide a complete understanding of how this neural network operates, although some interesting local connections (so-called 'motives') were identified [94, 95].

It became clear that the structure of neural networks can not be properly understood until their dynamics, ability, in principle, to change the structure is elucidated. In neuroscience, new terms, such as 'dynome' [96] and 'chronnectome' [97], were coined to describe the relationship between the network structure and dynamics. It became clear that the functional connectome is not identical to the anatomical connectome. The manifestation of one dynamic mode or another in the anatomical connectome depends on neuromodulators [78] released together with neurotransmitters near synapses. Unlike neurotransmitters, neuromodulators can diffuse over long distances. In addition, they can be liberated from specialized neuroendocrine cells lacking synaptic contacts. They can be transported around the body like hormones. The time of their action can be both relatively short (seconds or minutes) and long (hours) [98]. In other words, an anatomical connectome is a set of potential configurations of connections between neurons (or neural networks), whereas the real functional configuration depends on neuromodulators. Moreover, neuromodulators can qualitatively change the properties of neurons by transferring them, for example, from the tonic spike mode to the excitable stationary regime [98].

The term 'chronnectome' implies that the neural network of the brain changes in time, with alterations in both the activity of individual neurons and their connectivity (functional connectivity). A relatively new research subject has emerged, defined as 'adaptive dynamic networks' [82], i.e., those networks whose topology (connectivity) is rebuilt over time. Naturally, a question arises about the laws of such restructuring. In real neural networks, neuromodulators (and not them alone) are responsible for the restructuring, whereas, in 'mathematical' networks assembled from phase oscillators, the restructuring of connections is described mathematically [99–101] as a function of the strength of the connection between the network nodes of the current phases of these oscillators. In such models, it remains unclear how the mathematical rules for the restructuring of connections correlate with molecular processes in real networks.

Understanding the important role of plasticity (or adaptability) of neural networks promoted the understanding of the inevitability of self-structuring in neural networks. Ideas arose about the brain as a multiscale network system [88], about hub neurons that connect different functional areas of the brain [102], and about the hierarchy of neural networks [103]. One of the options for hierarchy is the modern theory of multilayer neural networks [104]. The mathematical apparatus for describing and analyzing the dynamics of networks of coupled oscillators, including oscillatory neural networks, is presented by Professor Ashwin in Ref. [105].

Finally, it is worth noting that neural networks are essentially the networks of spike oscillators with chemical synapses (given that electrical synapses are disregarded). Therefore, the long-standing interest in networks of spike oscillators [106] has recently grown even more than ever before [107–109]. Sometimes, spike neural networks are referred to as the third generation of artificial neural networks [108]. Note also that scientists engaged in cognitive research are calling for a greater integration between neuroscience and artificial intelligence (AI) [104]. One of the incentives for this is the fact that modern AI devices consume quite a lot of power, while spike oscillator networks are much more energy efficient. For example, Microsoft has developed the True-North chip, which operates based on the same principles as networks of spike neurons [110]. It consumes about 70 mW to perform 46 billion 'synaptic operations per second per watt.' Such power consumption is roughly four orders of magnitude lower than that of a conventional computer.

Because it is rather difficult to work with networks of oscillators described by complete models of real processes, researchers have to use a technique for reducing such systems to networks of phase oscillators. Recently, two excellent reviews have appeared in which reduction methods are described in full and systematically [111, 112]. For completeness of the description of neural networks, it is necessary to mention about such phenomenon as a chimera. This word denotes such a dynamic mode of the network in which some oscillators oscillate in phase while others exhibit asynchronous (chaotic) behavior. A recent review, Ref. [113], allows me to drop a description of this important behavior of neural networks.

Numerous studies on spike neural networks bring disparate information. Putting the pieces of the puzzle together into one big picture is not yet possible. To exemplify such a piece of information, suffice it to cite only one study [114] showing that strong inhibitory connections contribute to the maintenance of working memory. What to do next with this and similar information is a problem facing the researcher. Hopefully, working with small neural networks will allow us to come closer to understanding how the brain operates.

Finally, it should be mentioned that artificial spike neural networks are widely used in AI devices [115–121]. However, since we are describing the 'chemical brain' that works without electricity and without mathematical formulas, artificial intelligence schemes are not considered in the present review.

## 4. Microoscillators based on the Belousov–Zhabotinsky reaction

The BZ reaction has been studied perfectly well [9, 10]. It involves oxidation of malonic acid (although other substrates can be used) with bromate in an acidic medium, the process being catalyzed by metal ions or their complexes. The most commonly used catalysts are such metal complexes as ferroin, $Fe(phen)_3^{2+}$, or $Ru(bpy)_3^{2+}$. In a certain (very wide) range of concentrations of the initial reagents, this reaction proceeds in an oscillatory mode with fast autocatalytic oxidation of the catalyst, followed by its relatively slow reduction, after which the process is repeated.

The universally recognized mechanism of the BZ reaction is the Field–Köres–Noyes (FKN) mechanism [122] that includes 12 'elementary' reactions (see also [63]). When $Ru(bpy)_3^{2+}$ is used as the catalyst, the BZ reaction becomes photosensitive [123]. Depending on bromate ($BrO_3^-$) and malonic acid (MA) concentrations, light either inhibits oscillations (at high MA and low bromate levels) [124] or activates the autocatalysis and accelerates oscillations (at low MA and high bromate levels) [125].

The most important intermediates of the BZ reaction are bromide ($Br^-$) inhibiting oscillations and $HBrO_2$ activating them. In addition to $Br^-$, molecular bromine ($Br_2$) also inhibits oscillations; it is present in approximate equilibrium with bromine due to fast reactions in which $Br_2$ is converted into $Br^-$ and vice versa. Recall that autocatalysis in the BZ reaction begins when the concentration of inhibitor $Br^-$ falls below the critical threshold level [122, 126].

To complete the picture, it should be noted that the BZ reaction can exhibit birhythmicity [127] and chaotic oscillations [128–130], as well as stationary dissipative Turing structures [38], antiwaves [33], packet waves [34], and many other dissipative structures and waves [32, 126]. The dynamics of an oscillatory BZ reaction can resemble those of a neuron with its spikes, the only difference being the period of oscillations of the BZ reaction lies in the minute range, while neuron oscillations occur with a much higher frequency.

In the last decade, BZ MOs have gained interest in nonlinear chemistry (see Ref. [63]). Their use made possible experiments with a relatively large number of coupled chemical oscillators [41, 48, 49, 131–135].

As a rule, the diameter of such MOs varies from several ten to several hundred micrometers. On the average, a microoscillator can be represented as a microdroplet or a microsphere about 100 μm in diameter. BZ microspheres can be made (synthesized) from organic polymers, e.g., from an ion-exchange resin [134] or silica gel (an inorganic polymer) [136] with a catalyst for the BZ reaction immobilized in these microspheres. If such a BZ microsphere is immersed in a catalyst-free BZ solution (BZC solution), then the microspheres begin to oscillate as localized MOs. Because the initial

reagents of the BZ reaction (bromate and malonic acid) continuously diffuse from BZC into BZ microspheres, the oscillations persist for tens of hours without noticeable signs of amplitude alteration [136]. Such a BZ MO is suitable for creating networks of oscillators with stable modes.

BZ microdroplets are usually obtained by the microfluidic technique [40, 41, 137], because mixing the aqueous phase with an immiscible liquid (oil) results in microdroplet formation in a microhydrodynamic chip. The use of a BZ solution instead of pure water for mixing with oil yields BZ microdroplets in a continuous oil phase. The size of BZ droplets, like that of BZ microspheres, can be varied in a range from several ten to hundreds of micrometers.

## 5. Pulse coupling

Along with the methods for creating MOs, a pulsed coupling technique with a time delay was experimentally developed and implemented [64, 65, 138–143]. As applied to two relaxation BZ oscillators with indices $i$ and $j$, the pulse coupling with a delay looks like that shown in Fig. 1. If spike S occurs in oscillator $i$, it activates, after a time delay $\tau$, a mechanism of pulse impact on oscillator $j$. In the case of macrooscillators (macroreactors), this impact may have the form of a short-term injection of a small portion of a certain substance (activator or inhibitor) into reactor $j$. As far as microreactors are concerned, the impact can be targeted pulsed photoirradiation of a concrete MO (with number $j$ in the case of interest). The effect of such a coupling with a time delay is not described by delay differential equations [144, 145] in which the state of the system at any time $t$ affects the same or another system at time $t+\tau$. In the case of synaptic connections between neurons and in the case of the pulse coupling under consideration, only one (excited) state of the system (spike) at a given instant $t_0$ affects other neurons (oscillators) at time $t_0+\tau$. In neural networks, the time delay $\tau$ is mainly determined by the time of passage of the action potential along axons.

If the coupling is an inhibitory type, the pulse that arrives at oscillator $j$ 'postpones' the appearance of the next spike in this oscillator. In contrast, if the incoming pulse is an activator, it accelerates the onset of the spike in the $j$-oscillator. This coupling is sometimes called exciting. There is a very simple and effective way to characterize a pulse action with time delay by using phase response curves (PRCs) [147, 148].

Let the oscillator phase $\phi$ grow linearly with time and vary from 0 to 1, where unity corresponds to the total (from spike to spike) period $T$. On reaching 1, the phase is reset to zero. Let us express the moment of pulse perturbation in units of phase $\phi$ of the limit cycle as $\phi_p = \tau/T$, where time $\tau$ is counted from the instant of the previous spike to the moment of pulse perturbation. Then, the dependence of the phase shift $\Delta\phi = (T_n - T)/T$ on $\phi_p$ is the PRC, where $T_n$ is the time interval from the previous to the next spike provided that a single pulse perturbation of the oscillator occurs during this time, with the amplitude and pulse duration remaining unaltered with a change in phase $\phi_p$. Typical dependences of $\Delta\phi$ on $\phi$ (the subscript 'p' is omitted) for inhibitory and activatory (excitatory) pulse impacts on the BZ reaction are presented in Fig. 2 [149, 150].

The convenience of PRC lies in the possibility of describing a dynamic system (network) with pulse couplings between oscillators by a sequence of discrete events. Various

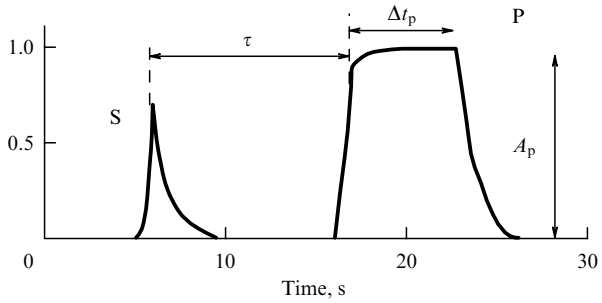


**Figure 1.** Pulse P in reactor $j$ occurs $\tau$ seconds after some variable S in reactor $i$ generates a spike and reaches a certain critical value. Almost rectangular pulse P is of duration $\Delta t_p$ and has amplitude $A_p$. (Borrowed from [146]).

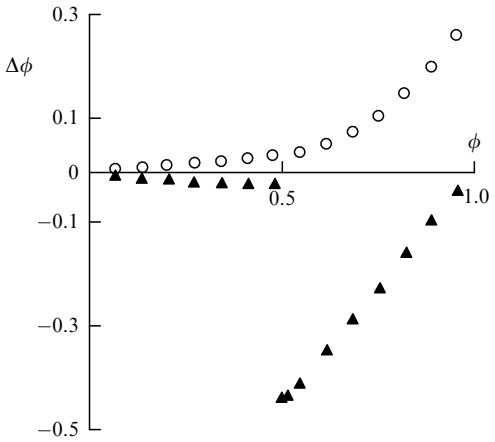


**Figure 2.** Typical inhibitory PRC (circles) and excitatory PRC (triangles) obtained in an experiment with the oscillatory BZ reaction. Curves are plotted based on data presented in [149].

aspects related to the stability of such a system, the slope of the PRC, and the sign of the second derivative of the PRC are described in Ref. [107].

## 6. Coupled BZ microoscillators

Let us consider the difference between diffusive coupling and pulse coupling using the example of two BZ MOs. Note that, for macrooscillators, diffusive coupling in its pure form is difficult to substantiate, and experimenters use mass transfer [151] instead, the effect of which differs markedly from diffusive coupling.

The excitatory or predominantly excitatory diffusive coupling is exemplified by the behavior of two BZ microspheres with an immobilized catalyst that are placed in an aqueous BZC solution (i.e., a BZ solution without a catalyst) [136]. At a large distance, their phases and frequencies are not synchronized (Fig. 3a). As BZ MOs approach one another (Fig. 3b, c), an excitatory coupling forms between them, which equalizes oscillation frequencies of the MOs and eventually leads to in-phase oscillations.

The inhibitory diffusive coupling is illustrated via an example of the behavior of two silica gel BZ microspheres preliminarily saturated with reagents of the BZ reaction and thereafter placed in the oil phase in which only hydrophobic molecules of the $Br_2$ inhibitor can diffuse [136]. Figure 4 shows that BZ MOs initially located at a large distance from

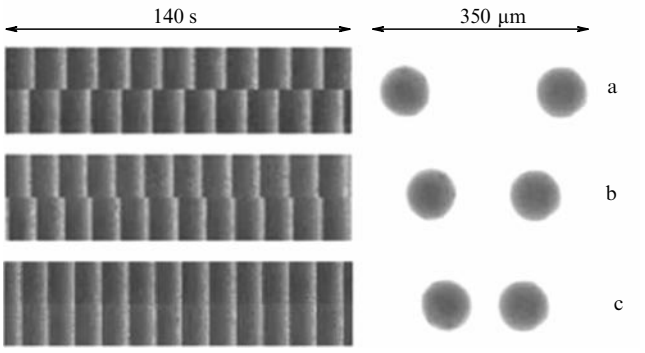


**Figure 3.** In-phase synchronization emerges as two BZ MOs connected via excitatory diffusive coupling approach each other. Silica gel microspheres were used. On space-time graphs, time moves from right to left, and optical transmission was recorded through a microscope in the central regions of the microspheres.

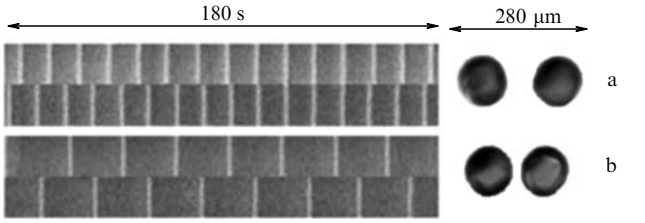


**Figure 4.** Antiphase synchronization emerges as two silica gel BZ MOs connected by inhibitory diffusive coupling approach each other. On space-time graphs, time moves from right to left, and optical transmission was recorded through a microscope in the central regions of the microspheres.

each other are not synchronized and oscillate with slightly different periods and phase shifts (Fig. 4a). However, an inhibitory coupling begins to form between them as they approach one another (Fig. 4b), which lengthens (almost twofold) and equalizes MO periods and ultimately leads to antiphase oscillations. Thus, the excitatory diffusive coupling gives rise to in-phase oscillations, while the inhibitory diffusive coupling generates out-of-phase oscillations.

A totally different behavior is observed for pulse coupling [64, 152]. First, the dynamic regime depends on two parameters: time delay $\tau$ and pulse amplitude $A_p$ at a constant pulse duration $\Delta t_p$ (see Fig. 1). Figure 5 shows regions of different dynamic modes for inhibitory (Fig. 5a) and excitatory (Fig. 5b) couplings on the $A_p - \tau$ plane. These diagrams were obtained for the theoretical model in [152], but qualitatively similar diagrams are possible to obtain in experiment [64]. Pulse amplitudes $A_p$ for the inhibitory and excitatory couplings are designated $C_{inh}$ and $C_{ex}$, respectively.

It follows from Fig. 5a that there is no region of exclusively antiphase oscillations for the inhibitory pulse coupling. Instead, there is a birhythmic region for relatively small $C_{inh}$ or $\tau$ (lower-left corner of the diagram in which either the AP or IP mode can appear, depending on the initial conditions, i.e., the oscillator phase ratio). But the most surprising thing is that only in-phase (IP) oscillations exist for relatively large $C_{inh}$ or $\tau$ (upper-right corner of the diagram). In the region of excessively large pulse amplitude, one of the oscillators may be completely suppressed (OSI region).

Figure 5b demonstrates no less interesting dynamic modes. First, there are no ideal in-phase oscillations in any region on the $C_{ex} - \tau$ plane as in the case of an excitatory diffusive coupling. At relatively small $C_{ex}$ and $\tau$ ($\tau$ is small with respect to the period of natural oscillations $T_0$, which corresponds to the lower left corner of the diagram), so-called almost in-phase oscillations (AIPs) are observed with the time shift between closely spaced oscillator spikes roughly equal to time delay $\tau$ and oscillation period $T$ approximately equal to $T_0$. As $\tau$ or $C_{ex}$ increase, a sudden transition from the AIP mode to the new fast antiphase mode (FAP) occurs). After time delay $\tau$, a pulse from one oscillator instantly causes a spike in the other oscillator and vice versa. Thus, the oscillation period is $T \cong 2\tau$. At very large $C_{ex}$, an OSII mode is formed in which one oscillator is in a stationary excited state and the other continues to oscillate as an independent oscillator with period $T_0$. There is a narrow area B between the regions of the OSII and FAP modes where bursting oscillations occur, which looks like trains of high-frequency spikes separated by periods of rest.

Thus, pulse coupling is not only an energetically advantageous way of 'communication' between oscillators but also a way to obtain new dynamic regimes that are absent in the case of diffusive coupling.

## 7. Small networks of spike oscillators

Let us now consider small networks of spike oscillators consisting of only a few nodes (oscillators or excitable cells).

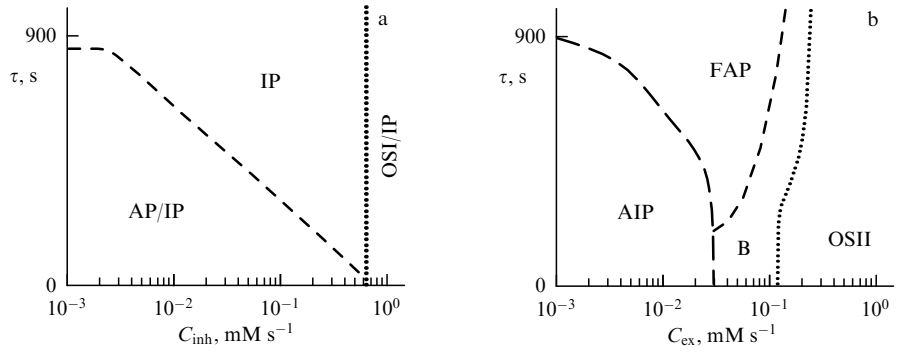


**Figure 5.** Diagrams of dynamic modes. (a) In plane $C_{inh} - \tau$ for inhibitory pulse coupling and (b) in plane $C_{ex} - \tau$ for excitatory pulse coupling. Symbols: IP — in-phase oscillations, AP — antiphase oscillations, OSI (OSII) mode implies that one oscillator is completely suppressed and is in a reduced (oxidized) state, FAP — fast antiphase oscillations, AIP — almost in-phase oscillations, B — bursting. Natural oscillation period $T_0$ of an isolated oscillator is 2150 s. Diagrams are constructed using data from Ref. [152].

Because we do not aim to provide a comprehensive mathematical description of such networks (as is fairly well done in Refs [81,107]), suffice it to focus here on those properties of these networks that can be used to create 'intelligent' autonomous devices. These properties include, first and foremost, clustering/synchronization and multirhythmicity. A large number of papers and even special issues of the journal *Chaos* [153, 154] have been devoted to these phenomena. In this context, clusters are groups of oscillators that oscillate synchronously. Networks of almost identical oscillators can have quite a few clusters. It is possible to count the number ($n$) of different states of a network of $N$ almost identical coupled oscillators. For $N = 2$, there are two stable symmetric states: in-phase and antiphase oscillations (see Fig. 5). Two oscillators in an in-phase state form a cluster. If $N = 3$, three states can be counted, viz. the in-phase mode, with all oscillators oscillating synchronously, the Splay mode, when the oscillators spike alternately with the time interval $T/n$ (where $T$ is the common period), and the '$2 + 1$' mode, when two oscillators oscillate synchronously while the third one is in antiphase to them. If account is taken of concrete synchronously oscillating oscillators (i.e., of permutations), the number of type '$2 + 1$' states goes to three, and the total number of states $n$ amounts to 5. For $N = 10$, taking into consideration permutations and combinations increases the number of states from $n = 40$ to $n = 487{,}311$ (by more than 4 orders of magnitude).

Accounting for states that differ from one another only in permutations (replacements) of the oscillators included in them is extremely important for the theory of heteroclinic transitions [155–159]. The group of Professor Timme, jointly with Professor Rabinovich's, also actively developed the theory of heteroclinic transitions in relation to the functioning of the brain and, accordingly, attached great importance to the permutations (replacements) of elements within clusters [160–162].

The dependence of the number of states $n$ on the number of elements (nodes) of the network $N$ is shown in Fig. 6 for two cases: with and without permutations (replacements).

If the permutations are disregarded, the number of states $n$ (for small $N$, e.g., $N < 8$) grows exponentially as $n \cong 0.44 \times 2^{0.63N}$ (the dependence indicated by diamonds in Fig. 6). But at $N > 10$, the growth of $n$ slows down and becomes linear (with a slope of 14.5). If the number of different states needs to be increased, it makes sense to break large networks into smaller ones, for example, for the number of states $n = 69$ and 11 for $N = 12$ and 6, respectively. Therefore, for a combination of two small networks with $N = 6$, the total number of modes, i.e., states, may be as large as $11^2 = 121$ or much more than $n = 69$.

Taking into account permutations leads to a multiple rise in the number of different states, and $n$ begins to grow approximately as $2^{2.5N}$ (the dependence indicated by red circles in Fig. 6). Note that the number of states $n$ in a group of unconnected cells, each capable of taking only two states (e.g., 0 and 1), grows as $2^N$, in contrast to the slower growth of the number of states $n$ (as $2^{0.63N}$) if permutations are disregarded. However, taking the permutations into consideration results in the growth of $n$ approximately as $2^{2.5N}$, i.e., much faster than that of the number of states in a group of uncoupled cells.

An example of symmetric regular dynamic modes for four oscillators coupled via inhibitory pulse coupling with a delay is presented in Fig. 7. The words 'symmetric regular' mean

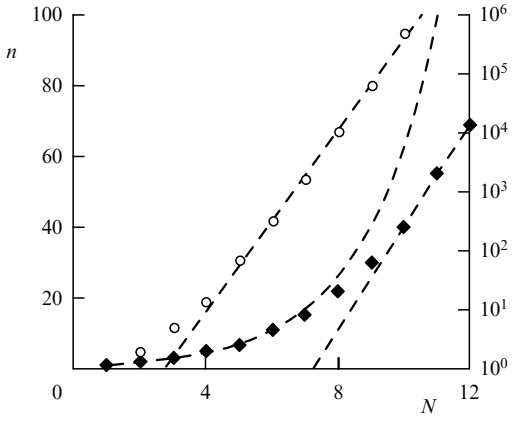


**Figure 6.** (Color online.) Dependence of the number of states ($n$) on the number of almost identical coupled oscillators ($N$). Blue diamonds mark the number of states without regard for permutations and combinations (left vertical axis), while red circles (which refer to the right logarithmic scale) denote the number of states $n$ taking into account permutations and combinations.

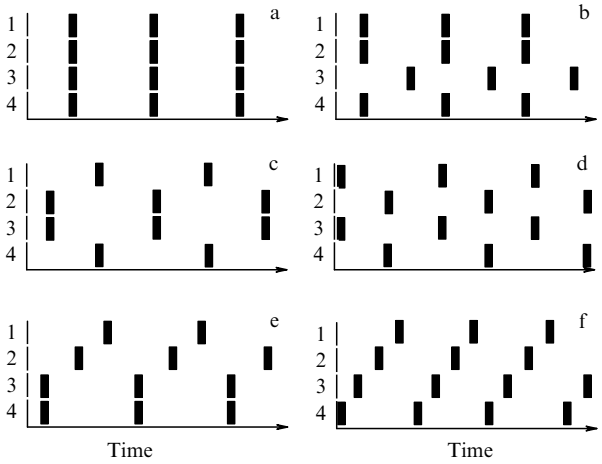


**Figure 7.** Regular dynamic modes found in a system of four spiked BZ oscillators, connected to each other by inhibitory pulse couplings with a time delay: (a) in-phase mode, (b) '$3 + 1$' cluster, (c) '$2 + 2$' cluster, IPAP mode, (d) '$2 + 2$' cluster, AP mode (antiphase oscillations), (e) '$2 + 1 + 1$' cluster, (f) step or Splay mode ('$1 + 1 + 1 + 1$' cluster). Short bold vertical strokes denote oscillator spikes, the numbers of which are shown to the left of the space-time graphs [163].

that each oscillator generates only one spike (regular oscillations) during one full period and that all oscillators have similar dynamics (symmetric oscillations).

There are other stable modes in addition to symmetric regular ones. Some of them are shown in Fig. 8. As a rule, such asymmetric modes appear when the pulse coupling is sufficiently strong [75].

When a network of oscillators has a large number of dynamic modes, the phenomenon of multistability often takes place, i.e., the coexistence of various stable states (modes or attractors) with the same set of system parameters. The implementation of one mode or another depends in this case only on the initial conditions [154]. Our calculations and experiments with small networks of pulse-coupled BZ oscillators show that multistability as a rule increases with increasing coupling strength [75, 141, 164].

Small networks consisting of only two or three quasi-identical pulse-coupled oscillators can have dozens of different modes and exhibit a high degree of multirhythmi-

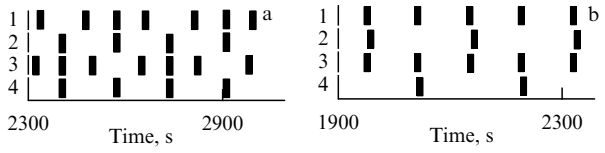


**Figure 8.** Asymmetric modes detected in a system of four BZ spike oscillators. (a) Oscillator nos 2 and 4 oscillate synchronously and produce two spikes for a common period, oscillator nos 1 and 3 produce three spikes for one common period and oscillate in antiphase. (b) Oscillator nos 1 and 3 oscillate synchronously and give two spikes during one common period, while oscillator nos 2 and 4 exhibit antiphase behavior and give one spike per period [75].

city if the amplitudes and delays of pulse signals are properly selected [165]. Thus, they are called 'cognitive modes,' which are highly sensitive to external impacts and at the same time resistant to small perturbations/noises.

A large number (tens) of different modes were identified theoretically when considering both one and two identical BZ MOs enclosed in a small capsule with impenetrable walls [166]. Such BZ MOs proved to be diffusively coupled. It turns out that the dynamic behavior of a pair of BZ MO inside the capsule strongly depends on the distance between MOs and even on the position of the pair in the capsule. Complex oscillations with alternating large and small peaks, various types of chaotic oscillations, and a stationary regime (suppressed oscillations) were detected, while an isolated BZ MO demonstrated ordinary regular oscillations.

Various dynamic modes, especially those associated with the formation of clusters in oscillator networks, are of importance, because different modes can serve as neural network memory, e.g., associative memory. Indeed, any stable dynamic mode is an attractor to which phase trajectories belonging to the basin of this mode converge. In complex networks, the attractor basins may have highly intricate and difficult to accurately define boundaries [167]. However, it is qualitatively understandable that small distortions of the input signal that do not leave the basin of a given mode will eventually lead to the same most stable mode.

Multirhythmicity of the central pattern generator (CPG) allows many animals to control the movements of their limbs and contraction of the stomach wall by switching from one mode to another [168–171]. A large number of studies have been devoted to the methods of switching between modes (see Refs [163, 172] and references therein). We have developed a special small block of cells called a reader (R) to identify concrete dynamical modes of CPGs [61, 163]. Knowing the current CPG rhythm and the final (desired) mode allows us to select pulses that 'correctly' switch CPGs.

The well-known neurophysiologist Buzsaki argues that a rationally organized neural network must have a special reading system to read out information from another special part of the neural network called the CPG or receiving unit [173]. In other words, any information entering the brain makes sense only when some of its other subsystems (the reader) can read and understand it [173]. The reader, in turn, sends this information to the integrator collecting information about external signals and the state of its own neural network. Thus, we move on to hierarchical networks containing various functional blocks that consist of spike oscillators or excitable cells. At the same time, the chemical nature of all microcells remains exactly the same: it is the BZ reaction that can proceed in different regimes.

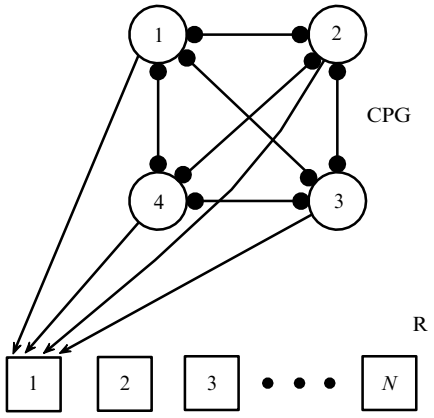


**Figure 9.** Neural-like hierarchical network represented by two blocks: CPG (central pattern generator) and R (reader). Four oscillators of the CPG block are connected 'each to each' by inhibitory pulse couplings. Cells of the R block are in a stationary excitable state and are waiting for excitatory pulses from the CPG block. Only pulse couplings between all oscillators of the CPG block and cell no. 1 of the R block are depicted so as not to overload the figure, but exactly such couplings exist for all other cells of the R block.

The operation of the reader in a generalized form is illustrated by Fig. 9. There are several ways to customize reader cells to various modes of the CPG block, e.g., the regular modes shown in Fig. 7. It is possible to sum the amplitudes of all pulses coming from CPG cells to each reader cell provided that these pulses arrive at the reader cells immediately after the spikes of the CPG block oscillators, which corresponds to zero delay. If all delays are equal, the result will be the same. Another condition is equal amplitudes of all pulses.

Next, one can configure the reader cells so that they have different spike excitation thresholds. For BZ MOs with the $Ru(bpy)_3^{2+}$ complex, different thresholds are achieved by simply increasing the intensity of constant illumination of the desired MO. The thresholds of cell nos 1, 2, and 3 can be made such that they will fire only when four, three, and two pulses, respectively, arrive at them simultaneously. The remaining cells (if any) can be triggered by single pulses. Obviously, the total maximum amplitudes will be different for the IP mode, the '3 + 1' cluster mode, and '2 + 2' cluster modes. Cell no. 1 and all other cells will respond to the IP mode. Cell no. 1 will no longer respond to the '3 + 1' mode, whereas all other cells will produce spikes. Cell no. 1 and no. 2 will not respond to the '2 + 2' and the '2 + 1 + 1' modes, but all other cells of the reader will give spikes. Thus, it will be impossible to distinguish between '2 + 2' and '2 + 1 + 1' modes, and even more so, between the AP (Fig. 7d) and IPAP modes (Fig. 7c).

Reader cells can be tuned to the frequency of pulses coming to them. This approach also has advantages and disadvantages [163]. The question of how a neural network encodes and decodes information is one of the central ones in neuroscience [174]. A common method for encoding information by a neural network is phase coding [108]. A special case of the method being considered is information encoding based on the synchronization of neuron spikes [175]. In our case, the phase encoding method in which pulses from different CPG oscillators arrive at the reader cells synchronously also proved most sensitive to different modes.

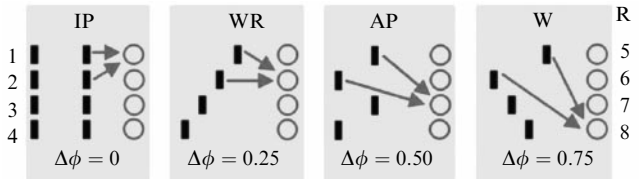


**Figure 10.** Figure illustrates the phase method of reader cell work. See the text for explanations. Numbers of CPG cells (left) are the same as in Fig. 9, and the four reader R cells (right) are numbered from 5 to 8.

The idea of the method under discussion is illustrated in Fig. 10. Pulses from cell no. 1 and no. 2 of the CPG block must reach definite cells of the reader at the same time, since all these cells produce a spike only in response to two simultaneously arriving pulses. In this case, we consider, for simplicity, the CPG block in which all oscillators are connected in a circle by unidirectional inhibitory pulse couplings.

This CPG block has four regular modes, viz. IP (in-phase), WR (walk reverse), AP (antiphase), and W (walk), shown in Fig. 10. Because the difference between phases of oscillator no. 1 and no. 2 is different for all four modes, time delays corresponding to the phase difference in different modes must be introduced if simultaneous arrival of pulses at cells 5–8 of the reader block is to be ensured. So, for the IP mode and cell no. 5 tuned to it, the time delay is zero. For the WR mode and cell no. 6 tuned to it, the time delay should be equal to a quarter of the oscillation period of the WR mode. For the AP and W modes and the corresponding cells 7 and 8, the time delay should be equal to half and 3/4 of the oscillation periods of either mode, respectively.

## 8. Principles of operation of the 'chemical brain'

Before demonstrating in practice how a hierarchical network of pulse-coupled oscillators and excitable cells can mimic intelligent behavior, let us briefly consider the principles or properties that such a network borrows from dynamical systems and biological neural networks. The following properties of dynamic systems are currently of interest for us: (a) oscillatory (limit cycle) and excitable states of a dynamic system (BZ oscillator); (b) adjustable excitation thresholds for cells in standby mode; (c) clustering of ensembles of almost identical coupled oscillators, (d) multistability or multirhythmicity, which is equivalent to the presence of several stable attractors. (Note that multistability is also inherent in neural networks, and there is an opinion that time delays in neural networks contribute to the creation of multistability [176]); (e) switching between stable attractors under the action of short external pulses; (f) the presence of attractors allows for some 'inaccuracy' in both switching between attractors and perceiving external information.

In our case, an external signal (i.e., information) activates one of the possible attractors of the receiving device (antenna) that is initially in a stationary standby mode. Our antenna does not work like a camera and does not remember all the details of the external signal. On the contrary, the external signal is transformed in the antenna into one of the possible attractors to which this signal is closest. The more attractors the antenna contains, the more accurate the perception of the external signal should be.

As far as biological principles underlying the organization of neural networks are concerned, we use the following ones:

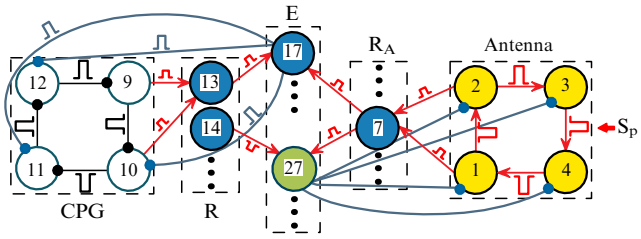


**Figure 11.** (Color online.) Schematic diagram of 'chemical brain.' Antenna block includes excitable cell nos 1–4. Reader block for the antenna ($R_A$) consists of excitable cell nos 5–8 (only cell no. 7 is shown). CPG block consists of oscillator nos 9–12. Reader for CPG (R) consists of excitable cell nos 13–16. Excitable cell nos 17–30 form block E (executer). Inhibitory pulses are indicated by segments or arcs with a small dot at the end, excitatory pulses by sections with an arrow at the end. $S_p$ denotes external signals (pulses) that can arrive at any antenna cell [62].

(a) network hierarchy; (b) compression of the original information; (c) replacement of an original external signal by its image, by analogy with the substitution of a word in our mind for real objects and actions; (d) feedback; (e) unidirectional information flow between some blocks achieved by using pulse couplings; (f) energy saving through the use of spike oscillators; (g) mutual inhibition of neurons (cells) that must not work simultaneously.

Putting together all the blocks described above yields a diagram of the 'chemical brain.' In this case, this is a network of pulse-coupled MOs simulating adaptability to external signals [62 ,77]. The scheme is presented in Fig. 11.

The CPG block consists of four BZ MOs connected in a circle via inhibitory pulse couplings. Such a CPG topology allows it to have four stable regular modes (see Fig. 10). The *antenna* block likewise consists of four BZ microcells in an excitable state. They are also connected in a circle, but by excitatory pulse couplings. Moreover, this block has the same four stable regular modes that are shown in Fig. 10. The numbers of modes in CPG and antenna blocks are purposely made to coincide to avoid the problem of choosing which antenna mode should be imitated in front of the CPG block. Readers R and $R_A$ read the state of the current modes of the CPG and antenna blocks, respectively. Only one cell is activated in each reader.

For definiteness, consider the case when the AP mode appeared in the antenna (such was the external signal $S_p$) and, accordingly, only one cell, no. 7, was activated; the current mode in the CPG block is the IP mode, and only one cell, no. 13, tuned to the IP mode is active in the reader R. We assume that our 'chemical brain' behaves reasonably if the current mode of the CPG block always corresponds to the antenna mode, i.e., the internal state of the device for which the CPG is responsible always adjusts to the external conditions recorded by the antenna. In this concrete case, our device must carry out the IP → AP switch.

The switching is done by the E block (executer) [61, 62], which must be able to switch any of the four modes of the CPG block to one of the other three modes at the request of the antenna. All cells of block E are in standby mode and can be activated by at least two simultaneously arriving pulses. Each activated cell of the E block sends three pulses to CPG cell nos 10–12 that implement switching between the given modes. Accordingly, the sets of these pulses are different for different transitions. To implement the considered IP → AP transition, only one cell of block E (no. 17) must be activated from active cell nos 7 and 13.

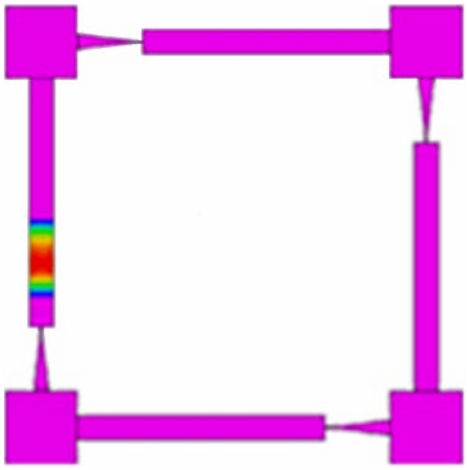

**Figure 12.** (Color online.) Four microoscillators (depicted as small squares in the corners of a large square structure) are connected by microchannels of a special shape to ensure the unidirectionality of chemical waves propagating through the channels. Area with the maximum concentration of the catalyst in the left channel along which the wave runs is marked in red.

As soon as the IP → AP transition has occurred, another cell, no. 14, responsible for recording the AP mode, is activated in block R. Now, two active cells, no. 14 and no. 7, activate another cell (no. 27) in block E. This cell (as well as similar cell nos 28–30) is intended to bring the antenna back to the stationary standby regime by sending inhibitory pulses to the antenna cells. This completes the switching operation and makes the device ready to receive new external signals.

At present, the scheme presented in Fig. 11 has already been implemented experimentally [62], but cell to cell pulse couplings are formed by means of irradiation of microcells with focused beams of light coming from a computer-controlled projector. Therefore, the overall size of the device depends on the size of the microscope, computer, and projector. However, one can do without these big tools if pulse couplings between cells are created in exactly the same way as in neurons, i.e., with the use of chemical waves propagating through narrow channels as shown in Fig. 12. This method provides all the modes in CPG and antenna blocks found earlier for optical pulse coupling.

## 9. Decision-making

In order for the MO network under consideration to be more like a 'chemical brain,' it must be able not only to adapt to external conditions according to a previously specified program (see the scheme in Fig. 11) but also to make independent decisions. A huge number of studies have been devoted to the problem of decision-making by an artificially created device. According to the Web of Science, there have been more than 12,000 reviews published over the past three years. Therefore, we refer here only to relatively recent reviews that we find interesting, important, and most closely related to our approach to the creation of a 'smart' device based on networks of coupled active elements [177–192].

Decision-making depends on many factors, such as the current state (both physical and emotional) of a given system or individual, information on previously acquired experience (memory), ideas about the future, social connections, chance factors, etc. The relatively small Drosophila brain (about 100,000 neurons) integrates in its central part information from many (peripheral) regions to make a decision about the direction of movement of this fly [181]. How decisions are taken under the uncertainty of the surrounding world and how Bayesian decision-making models work is discussed in reviews [182, 188] and [187], respectively. References [179, 190] are focused on the importance of the value of information for making decisions under conditions of external uncertainty and a multiplicity of decisions. The influence of emotions on decision-making and the role of rewards in the process of learning and decision-making are considered in reviews [185, 189], respectively; in the latter review, this problem is discussed at the level of concrete neurons and neural networks. Review [178] is devoted to the choice of the sole correct solution from a large number of options; the authors claim that they managed to single out six canonical biologically plausible schemes of neurons (mini-networks) universal for solving such problems.

How to use the latest achievements in research on artificial neural networks to solve neuroscience problems is discussed in review [183]. The relationship between artificial and natural intelligence is discussed in Ref. [184] in the context of solving multiscale problems with special reference to events at small and large spatial and temporal scales.

Trying to rethink and simplify the huge amount of information on decision-making mechanisms in relation to the 'chemical brain' concept being developed by our group, we proposed the simplest scheme of such a 'brain' (see Fig. 13). Figure 13a suggests that all information about the internal state of the 'chemical brain' expressed by the modes of the CPG block and about external (input) signals expressed by the modes of the antenna enters the decision-making block (DM) indirectly through the R and $R_A$ readers. For simplicity of the network under consideration, the CPG block has only two states (two modes): in-phase and antiphase oscillations. The antenna also has only two stable attractors (IP and AP).

The decision on whether the CPG block should match the mode in the antenna is made by the DM block, shown as a yellow square in Figs 13a and 13b. The decision is communicated to executing block E by cells 11–16, shown in Fig. 13b. Suppose that the IP mode arises in the antenna (cell no. 7 is active) and the AP mode exists in the CPG block (cell no. 4 is active). For some reason, the DM block decides to accept an external mode. Then, it activates the 'Pro' cell (cell no. 11) that will continue to maintain spike oscillations in itself by virtue of self-activation. The two active (oscillating) cells, no. 11 and no. 7, should activate cell 13 if pulses from these cells arrive at cell no. 13 simultaneously. Then, two active cells, nos 4 and 13, activate cell no. 9, which switches the CPG block from the AP mode to the IP mode. A similar way of reasoning holds for the remaining three combinations of AP and IP modes in CPG and antenna blocks.

The structure of DM blocks can be rather complicated. In the simplest case, a DM block retrieves information about previous switches from memory to make a decision or simply makes random decisions. Also, decisions can be made by comparing information originating from two or more antennas, i.e., different sources, that differently respond to an external signal, thus giving food for analysis to the decision block. We believe that DM blocks should be designed making use of the extensive information contained in the reviews [177–192] cited above jointly with a consulting neurophysiologist able to evaluate the biological essence of one scheme or another.

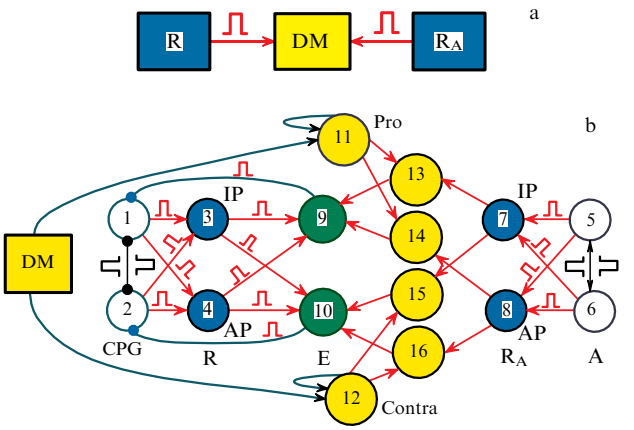


**Figure 13.** (Color online.) (a) Information from readers R and $R_A$ enters the decision-making block (DM). (b) Specification of signals between the cells of 'chemical brain' blocks. CPG block consists of microoscillators 1–2. Reader of this block is represented by cell nos 3 and 4. If the IP mode occurs in the CPG, cell no. 3 begins to generate periodic spikes; if the AP mode occurs, cell no. 4 starts to generate periodic spikes. Antenna consists of cells 5–6 and its reader of cells 7–8. Green cells, nos 9 and 10, represent the executing block E that switches or does not switch the CPG block to another mode. Block DM (shown in yellow) is divided into two parts; one is hidden (DM square in Figs a and b), the other is explicit (cells 11–16).

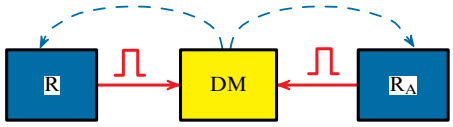


**Figure 14.** Information from readers R and $R_A$ enters the decision-making block DM that, in turn, can activate cells in the readers.

To conclude this section, let us explain why information about external and internal processes comes to the DM unit from readers but not directly from the antenna and CPG blocks. The fact is that active cells of the readers play the role of names of a concrete mode. Indeed, they introduce a symbolic language that can be used even when the main blocks, i.e., the antenna and the CPG, are turned off (sleep). Imagine that exciting pulses are sent from DM or any other blocks to readers R or $R_A$, as shown in Fig. 14. This can revive such blocks and enable them to replace real signals. As a result, the entire system sorts out possible consequences of making a decision; hence, a chance to foresee the future.

## 10. Conclusion

A A Zhdanov writes in his book *Autonomous Artificial Intelligence* that asomatous artificial intelligence is fundamentally different from the real intelligence of a living organism [193]. In this review, we have described basic principles of the 'chemical brain' partly borrowed from living organisms that have a nervous system. It makes our approach to the creation of the 'chemical brain' somewhat similar to that of A A Zhdanov, although he does not postulate any chemical MO. The difference between our 'chemical brain' and all other forms of AI is that it does not need electricity and can work using chemical fuel alone.

In addition, our 'chemical brain' is a dynamical system (a network of coupled oscillators and excitable cells) and therefore, unlike other AIs, makes extensive use of nonlinear dynamics principles. We use dynamic modes of networks and subnetworks of coupled oscillators for remembering information, for the symbolic language used in information exchange between various dynamic blocks of the 'chemical brain,' for the self-determination of its state by the system, and for decision-making. But there is still plenty to use. Hopefully, the 'chemical brain' will be made more perfect with further progress in AI as regards pattern recognition. The first successful steps toward the creation of a 'chemical brain' capable of adapting to external signals [62, 77] open up prospects for fruitful research and developments along this new path.

**Acknowledgements.** This work was supported by the Russian Foundation for Basic Research (grant no. 20-11-50011). The author considers it his pleasant duty to express gratitude to the organizers of the IKBFU-based Program for Improving the Competitiveness, — which prompted the idea to write this review.

## References

1. Raychowdhury A et al. *Proc. IEEE* **107** 73 (2019)
2. Parrilla-Gutierrez J M et al. *Nat. Commun.* **11** 1442 (2020)
3. Zhabotinsky A M *Proc. Acad. Sci. USSR* **157** 392 (1964); *Dokl. Akad. Nauk SSSR* **157** (2) 392 (1964)
4. Belousov B P, in *Sbornik Referatov po Radiatsionnoi Meditsine za 1958 g.* (Collection of Short Papers on Radiation Medicine for 1958) (Ed. A V Lebedinskii) (Moscow: Medgiz, 1959) p. 145
5. Nicolis G, Prigogine I *Self-Organization in Nonequilibrium Systems* (New York: Wiley-Interscience, 1977)
6. Prigogine I, Lefever R *J. Chem. Phys.* **48** 1695 (1968)
7. Gray P, Scott S K *Chemical Oscillations and Instabilities: Non-linear Chemical Kinetics* (Oxford: Clarendon Press, 1990)
8. Epstein I R, Pojman J A *An Introduction to Nonlinear Chemical Dynamics* (New York: Oxford Univ. Press, 1998)
9. Field R J, Burger M *Oscillations and Traveling Waves in Chemical Systems* (New York: Wiley, 1985)
10. Epstein I R, Showalter K *J. Phys. Chem.* **100** 13132 (1996)
11. Ivanitsky G R, Krinsky V I, Sel'kov E E *Matematicheskaya Biologiya Kletki* (Mathematical Biology of the Cell) (Moscow: Nauka, 1978)
12. Ivanitsky G R, Krinsky V I, Zaikin A N, Zhabotinsky A M *Biol. Rev. D* **2** 279 (1981)
13. Krinsky V I (Ed.) *Self-Organization: Autowaves and Structures Far from Equilibrium. Proc. of an Intern. Symp., Pushchino, USSR, July 18–23, 1983* (Springer Series in Synergetics, Vol. 28) (Berlin: Springer-Verlag, 1984)
14. Lengyel I, Rábai G, Epstein I R *J. Am. Chem. Soc.* **112** 4606 (1990)
15. Luo Y, Epstein I R *J. Am. Chem. Soc.* **113** 1518 (1991)
16. Rábai G, Orban M, Epstein I R *J. Phys. Chem.* **96** 5414 (1992)
17. Lee K J et al. *Science* **261** 192 (1993)
18. Edblom E C et al. *J. Am. Chem. Soc.* **109** 4876 (1987)
19. Edblom E C et al. *J. Phys. Chem.* **93** 2722 (1989)
20. Boissonade J, De Kepper P *J. Phys. Chem.* **84** 501 (1980)
21. Field R J, Noyes R M *J. Chem. Phys.* **60** 1877 (1974)
22. Epstein I R, Luo Y *J. Chem. Phys.* **95** 244 (1991)
23. Marsden J E, McCracken M *The Hopf Bifurcation and its Applications* (New York: Springer-Verlag, 1976)
24. Noszticzius Z e al. *Nature* **329** 619 (1987)
25. Castets V et al. *Phys. Rev. Lett.* **64** 2953 (1990)
26. Ouyang Q, Swinney H L *Nature* **352** 610 (1991)
27. Turing A M *Philos. Trans. R. Soc. Lond. B* **237** 37 (1952)
28. Zaikin A N, Zhabotinsky A M *Nature* **225** 535 (1970)
29. Perez-Munuzuri V et al. *Nature* **353** 740 (1991)
30. Zhou L, Ouyang Q *Phys. Rev. Lett.* **85** 1650 (2000)
31. Ouyang Q, Flesselles J M *Nature* **379** 143 (1996)
32. Vanag V K *Phys. Usp.* **47** 923 (2004); *Usp. Fiz. Nauk* **174** 991 (2004)
33. Vanag V K, Epstein I R *Science* **294** 835 (2001)
34. Vanag V K, Epstein I R *Phys. Rev. Lett.* **88** 088303 (2002)

35. Vanag V K, Epstein I R *Proc. Natl. Acad. Sci. USA* **100** 14635 (2003)
36. Vanag V K, Epstein I R *Chaos* **17** 037110 (2007)
37. Bansagi T, Vanag V K, Epstein I R *Science* **331** 1309 (2011)
38. Vanag V K, Epstein I R *Phys. Rev. Lett.* **87** 228301 (2001)
39. Vanag V K, Epstein I R *Phys. Rev. E* **71** 066212 (2005)
40. Toiya M, Vanag V K, Epstein I R *Angew. Chem. Int. Ed.* **47** 7753 (2008)
41. Toiya M, Gonzalez-Ochoa H O, Vanag V K, Fraden S, Epstein I R *J. Phys. Chem. Lett.* **1** 1241 (2010)
42. Maselko J, Showalter K *Nature* **339** 609 (1989)
43. Totz J F et al. *Phys. Rev. E* **92** 022819 (2015)
44. Totz J F et al. *Nat. Phys.* **14** 282 (2018)
45. Wilson D et al. *Chaos* **28** 123114 (2018)
46. Taylor A F et al. *Eur. Phys. J. Spec. Top.* **165** 137 (2008)
47. Taylor A F et al. *Science* **323** 614 (2009)
48. Taylor A F et al. *Angew. Chem. Int. Ed.* **50** 10161 (2011)
49. Tompkins N et al. *Proc. Natl. Acad. Sci. USA* **111** 4397 (2014)
50. Vanag V K, Epstein I R *Engineering of Chemical Complexity II* (Singapore: World Scientific, 2014) Ch. 10
51. Litschel T et al. *Lab Chip* **18** 714 (2018)
52. Norton M M et al. *Phys. Rev. Lett.* **123** 148301 (2019)
53. Gorecki J, Gorecka J N, Adamatzky A *Phys. Rev. E* **89** 042910 (2014)
54. Gorecki J *Entropy* **22** 313 (2020)
55. Adamatzky A *Philos. Trans. R. Soc. B* **374** 20180372 (2019)
56. Torbensen K et al. *J. Phys. Chem. C* **121** 13256 (2017)
57. Budroni M A et al. *J. Phys. Chem. Lett.* **11** 2014 (2020)
58. Yoshikawa K, Aihara R, Agladze K *J. Phys. Chem. A* **102** 7649 (1998)
59. Gorecki J, Yoshikawa K, Igarashi Y *J. Phys. Chem. A* **107** 1664 (2003)
60. Hamada T e al. *Langmuir* **21** 7626 (2005)
61. Smelov P S, Proskurkin I S, Vanag V K *Phys. Chem. Chem. Phys.* **21** 3033 (2019)
62. Proskurkin I S, Smelov P S, Vanag V K *Phys. Chem. Chem. Phys.* **22** 19359 (2020)
63. Mallphanov I L, Vanag V K *Russ. Chem. Rev.* **90** 1263 (2021); *Usp. Khimii* **90** 1263 (2021)
64. Horvath Vet al. *Angew. Chem. Int. Ed.* **51** 6878 (2012)
65. Horvath V et al. *Phys. Chem. Chem. Phys.* **17** 4664 (2015)
66. Ke H et al. *Phys. Rev. E* **89** 052712 (2014)
67. Kuramoto Y *Int. J. Bifurcat. Chaos* **7** 789 (1997)
68. Kuramoto Y *Physica D* **50** 15 (1991)
69. Kuramoto Y, Battogtokh D *Nonlin. Phenom. Complex Syst.* **5** 380 (2002)
70. Winfree A T *J. Theor. Biol.* **16** 15 (1967)
71. Kuramoto Y, in *Intern. Symp. on Mathematical Problems in Theoretical Physics, January 23–29, 1975, Kyoto Univ., Kyoto, Japan* (Lecture Notes Physics, Vol. 39, Ed. H Araki) (Berlin: Springer, 1975) p. 420
72. Hubel D H, Wiesel T N *J. Physiol.* **148** 574 (1959)
73. Hodgkin A L, Huxley A F *Proc. R. Soc. Lond. B* **140** 177 (1952)
74. Sakaguchi H, Kuramoto Y *Prog. Theor. Phys.* **76** 576 (1986)
75. Vanag V K, Smelov P S, Klinshov V V *Phys. Chem. Chem. Phys.* **18** 5509 (2016)
76. Watts D J, Strogatz S H *Nature* **393** 440 (1998)
77. Vanag V K *Chaos* **29** 083104 (2019)
78. Bargmann C I, Marder E *Nat. Meth.* **10** 483 (2013)
79. Bargmann C I *Bioessays* **34** 458 (2012)
80. Vanag V K, Epstein I R *Phys. Rev. E* **84** 066209 (2011)
81. Klinshov V V, Nekorkin V I *Phys. Usp.* **56** 1217 (2013); *Usp. Fiz. Nauk* **183** 1323 (2013)
82. Maslennikov O V, Nekorkin V I *Phys. Usp.* **60** 694 (2017); *Usp. Fiz. Nauk* **187** 745 (2017)
83. Gencay R, Liu T *Physica D* **108** 119 (1997)
84. Rosenblatt F "The perceptron — a perceiving and recognizing automaton", Report 85-460-1 (Buffalo, NY: Cornell Aeronautical Laboratory, 1957)
85. Rosenblatt F *Psycholog. Rev.* **65** 386 (1958)
86. Ermentrout B, Park Y, Wilson D *Philos. Trans. R. Soc. A* **377** 20190092 (2019)
87. Bassett D S, Sporns O *Nat. Neurosci.* **20** 353 (2017)
88. Bassett D S, Zurn P, Gold J I *Nat. Rev. Neurosci.* **19** 566 (2018)
89. Bassett D S, Khambhati A N, Grafton S T *Annu. Rev. Biomed. Eng.* **19** 327 (2017)
90. Markram H *Sci. Am.* **306** (5) 50 (2012)
91. Sporns O *Neuroimage* **80** 53 (2013)
92. Alivisatos A P et al. *Neuron* **74** 970 (2012)
93. White J G et al. *Philos. Trans. R. Soc. B* **314** 1 (1986)
94. Marder E, Taylor A L *Nat. Neurosci.* **14** 133 (2011)
95. Milo R et al. *Science* **298** 824 (2002)
96. Kopell N J et al. *Neuron* **83** 1319 (2014)
97. Calhoun V D et al. *Neuron* **84** 262 (2014)
98. Marder E *Neuron* **76** 1 (2012)
99. Kasatkin D V, Nekorkin V I *Radiophys. Quantum Electron.* **58** 877 (2016); *Izv. Vyssh. Uchebn. Zaved. Radiofiz.* **58** 981 (2015)
100. Botella-Soler V, Glendinning P *Phys. Rev. E* **89** 062809 (2014)
101. Maistrenko Y L et al. *Phys. Rev. E* **75** 066207 (2007)
102. van den Heuvel M P, Sporns O *Trends Cognitive Sci.* **17** 683 (2013)
103. Chaudhuri R et al. *Neuron* **88** 419 (2015)
104. Hernandez A, Amigo J M *Eur. Phys. J. Spec. Top.* **227** 1039 (2018)
105. Ashwin P, Coombes S, Nicks R *J. Math. Neurosci.* **6** 2 (2016)
106. Maass W *Neural Networks* **10** 1659 (1997)
107. Klinshov VV *Izv. Vyssh. Uchebn. Zaved. Priklad. Nelin. Dinamika* **28** (5) 465 (2020)
108. Tan C, Sarlija M, Kasabov N *Neural Proc. Lett.* **52** 1675 (2020)
109. Kiselev M V *Comput. Res. Model.* **12** 401 (2020)
110. TrueNorth (2021), https://www.research.ibm.com/articles/brain-chip.shtml
111. Kuramoto Y, Nakao H *Philos. Trans. R. Soc. A* **377** 20190041 (2019)
112. Pietras B, Daffertshofer A *Phys. Rep.* **819** 1 (2019)
113. Majhi S et al. *Phys. Life Rev.* **28** 100 (2019)
114. Kim R, Sejnowski T J *Nat. Neurosci.* **24** 129 (2021)
115. Stockel A, Eliasmith C *Neural Computat.* **33** 96 (2021)
116. Kim J et al. *Neurocomputing* **428** 153 (2021)
117. Demin V A et al. *Neural Networks* **134** 64 (2021)
118. She X Y et al. *Front. Neurosci.* **14** 615756 (2021)
119. Xing Y N, Di Caterina G, Soraghan J *Front. Neurosci.* **14** 590164 (2020)
120. Li X M, Yi H, Luo S Y *Neural Plasticity* **2020** 8851351 (2020)
121. Lu S, Sengupta A *Front. Neurosci.* **14** 535 (2020)
122. Field R J, Körös E, Noyes R M *J. Am. Chem. Soc.* **94** 8649 (1972)
123. Kuhnert L *Nature* **319** 393 (1986)
124. Kádár S, Amemiya T, Showalter K *J. Phys. Chem. A* **101** 8200 (1997)
125. Kaminaga A, Mori Y, Hanazaki I *Chem. Phys. Lett.* **279** 339 (1997)
126. Vanag V K *Dissipativnye Struktury v Reaktsionno-diffuzionnykh Sistemakh* (Dissipative Structures in Reactive Diffusion Systems) (Moscow: R&C Dynamics, 2008)
127. Taylor A F *Prog. React. Kinet. Mec.* **27** 247 (2002)
128. Hudson J L, Hart M, Marinko D *J. Chem. Phys.* **71** 1601 (1979)
129. Marchettini N et al. *Phys. Chem. Chem. Phys.* **12** 11062 (2010)
130. Turner J S et al. *Phys. Lett. A* **85** 9 (1981)
131. Nkomo S, Tinsley M R, Showalter K *Phys. Rev. Lett.* **110** 244102 (2013)
132. Tinsley M et al. *Physica D* **239** 785 (2010)
133. Taylor A F, Tinsley M R, Wang F, Huang Z, Showalter K *Science* **323** 614 (2009)
134. Taylor A F, Tinsley M R, Showalter K *Phys. Chem. Chem. Phys.* **17** 20047 (2015)
135. Markovic V M et al. *Chaos* **29** 033130 (2019)
136. Mallphanov I L, Vanag V K *J. Phys. Chem. A* **124** 272 (2020)
137. Delgado J et al. *Soft Matter* **7** 3155 (2011)
138. Lavrova A I, Vanag V K *Phys. Chem. Chem. Phys.* **16** 6764 (2014)
139. Proskurkin I S, Vanag V K *Russ. J. Phys. Chem. A* **89** 331 (2015); *Zh. Fiz. Khim.* **89** 340 (2015)
140. Smelov P S, Vanag V K *Russ. J. Phys. Chem. A* **91** 1015 (2017); *Zh. Fiz. Khim.* **91** 963 (2017)
141. Safonov D A, Klinshov V, Vanag V K *Phys. Chem. Chem. Phys.* **19** 12490 (2017)
142. Horvath V, Epstein I R *Chaos* **28** 045108 (2018)
143. Proskurkin I S, Smelov P S, Vanag V K *Chemphyschem* **20** 2162 (2019)
144. Murray J D *Mathematical Biology I. An Introduction* (New York: Springer, 2002)

145. DDE (2021), http://www.scholarpedia.org/article/Delay-differential_equations
146. Vanag V K "Svyazannye khimicheskie ostsillyatory" ("Coupled chemical oscillators"), in *Nelineinye Volny 2016* (Non-Linear Waves 2016) (Eds A M Sergeev, A V Slyunyaev) (Nizhni Novgorod: IPF RAN, 2017) p. 263
147. Achuthan S, Canavier C C *J. Neurosci.* **29** 5218 (2009)
148. Canavier C C, Achuthan S *Math. Biosci.* **226** 77 (2010)
149. Proskurkin I S, Lavrova A I, Vanag V K *Chaos* **25** 064601 (2015)
150. Proskurkin I S, Vanag V K *Phys. Chem. Chem. Phys.* **17** 17906 (2015)
151. Crowley M F, Epstein I R *J. Phys. Chem.* **93** 2496 (1989)
152. Safonov D A, Vanag V K *Phys. Chem. Chem. Phys.* **20** 11888 (2018)
153. Abrams D M, Pecora L M, Motter A E *Chaos* **26** 094601 (2016)
154. Feudel U, Pisarchik A N, Showalter K *Chaos* **28** 033501 (2018)
155. Rabinovich M I, Muezzinoglu M K *Phys. Usp.* **53** 357 (2010); *Usp. Fiz. Nauk* **180** 371 (2010)
156. Rabinovich M I, Afraimovich V S, Varona P *Dyn. Syst. Int. J.* **25** 433 (2010)
157. Rabinovich M I et al. *Front. Computat. Neurosci.* **8** 22 (2014)
158. Rabinovich M I et al. *Phys. Life Rev.* **9** 51 (2012)
159. Rabinovich M I, Varona P *Front. Computat. Neurosci.* **5** 24 (2011)
160. Neves F S, Timme M *J. Phys. A* **42** 345103 (2009)
161. Neves F S, Timme M *Phys. Rev. Lett.* **109** 018701 (2012)
162. Kirst C, Timme M, Battaglia D *Nat. Commun.* **7** 11061 (2016)
163. Smelov P S, Vanag V K *R. Soc. Open Sci.* **5** 171495 (2018)
164. Vanag V K, Yasuk V O *Chaos* **28** 033105 (2018)
165. Vanag V K *Chaos* **29** 033106 (2019)
166. Vanag V K *Chaos* **30** 013112 (2020)
167. Saha A, Feudel U *Chaos* **28** 033610 (2018)
168. Ryczko D, Simon A, Ijspeert A J *Trends Neurosci.* **43** 916 (2020)
169. Sanders R H, Levitin D J *Brain Sci.* **10** 215 (2020)
170. Mantziaris C, Bockemuehl T, Bueschges A *Develop. Neurobiol.* **80** 16 (2020)
171. Hachoumi L, Sillar K T *Develop. Neurobiol.* **80** 42 (2020)
172. Klinshov V, Nekorkin V *Commun. Nonlin. Sci. Num. Sim.* **83** 105067 (2020)
173. Buzsaki G *Neuron* **68** 362 (2010)
174. Brette R *Front. Syst. Neurosci.* **9** 151 (2015)
175. Buzsáki G, Freeman W *Current Opin. Neurobiol.* **31** v–ix (2015)
176. Asl M M, Valizadeh A, Tass P A *Sci. Rep.* **8** 12068 (2018)
177. ter Wal M et al. *Nat. Commun.* **11** 3075 (2020)
178. Mysore S P, Kothari N B *Elife* **9** e51473 (2020)
179. Busemeyer J R et al. *Trends Cognitive Sci.* **23** 251 (2019)
180. Bielczyk N Z et al. *Plos One* **14** e0211885 (2019)
181. Cheong H S J, Siwanowicz I, Card G M *Current Opin. Neurobiol.* **65** 77 (2020)
182. Monosov I E *Trends Neurosci.* **43** 795 (2020)
183. Yang G R, Wang X J *Neuron* **107** 1048 (2020)
184. Badman R P, Hills T T, Akaishi R *Brain Sci.* **10** 396 (2020)
185. Mendl M, Paul E S *Neurosci. Biobehavioral Rev.* **112** 144 (2020)
186. Tekulve J et al. *Front. Neurorobotics* **13** 95 (2019)
187. Ma W J *Neuron* **104** 164 (2019)
188. Soltani A, Izquierdo A *Nat. Rev. Neurosci.* **20** 635 (2019)
189. Cox J, Witten I B *Nat. Rev. Neurosci.* **20** 482 (2019)
190. Bolam F C et al. *Biol. Rev.* **94** 629 (2019)
191. Zhdanov A et al. *J. Comput. Syst. Sci. Int.* **47** 907 (2008)
192. Zhdanov A A *J. Comput. Syst. Sci. Int.* **38** 792 (1999)
193. Zhdanov A A *Avtonomnyi Iskusstvennyi Intellekt* (Autonomous Artificial Intelligence) (Moscow: Binom. Laboratoriya Znanii, 2020)
194. Proskurkin I S, Vanag V K *Phys. Chem. Chem. Phys.* **20** 16126 (2018)